Full Paper

A STUDY ON THE OPTIMIZATION AND ADSORPTION CAPACITY OF ACTIVATED CARBON PRODUCED FROM POLYVINYL CHLORIDE (PVC) WASTES

O.D. Alabi-Babalola
Department of Chemical Engineering, Obafemi Awolowo University, Ile-Ife, Osun-State, Nigeria.

E.F. Aransiola
Department of Chemical Engineering, Obafemi Awolowo University, Ile-Ife, Osun-State, Nigeria.
aransiolaef@gmail.com

T.D. Shittu
Department of Chemical Engineering, Obafemi Awolowo University, Ile-Ife, Osun-State, Nigeria.

ABSTRACT

Activated carbon (AC) was prepared by the pyrolysis of polyvinyl chloride (PVC) wastes. This was with a view to optimize and study its adsorption capacity through various activation processes. The optimization study was carried out using the central composite design of the response surface methodology (RSM). The effects of the reaction conditions: carbonization temperature (400 – 500 oC), concentration of chemical activating agents (0.50 – 2.00 M H2SO4 and KOH) and activation time (45 – 60 min) on the yield and other physicochemical properties were investigated. The study revealed that an optimum yield of 80 % was achieved at an average activation time of 48-50 min, and average temperature of 425-450 oC. Maximum adsorption capacity was obtained at optimized reaction conditions of 0.50 M, and 500 oC. However, the optimum time for both PVC-H2SO4 and PVC-KOH are 46.46 and 55.35 min respectively. Fourier transform infrared (FT-IR) analysis revealed the presence of oxygen-surface complexes such as the carbonyls and O-H groups on the surface of the AC which was due to chemical activation. Scanning electron microscope (SEM) analysis shows the presence of pores and cave-type openings on the carbon surface sites, thus, confirming the porosity in the carbons. The adsorption data was found to perfectly fit the Freundlich model at an adsorbent dosage of 0.75 g/100 mL of adsorbate. Equilibrium was reached between 60 and 75 min. The kinetic studies showed that the pseudo-second-order model provides the best correlation for the dynamic behaviour for the sorption of inorganic ions onto AC with a kinetic rate constant of 0.0178 min-1 and correlation coefficient of 0.9988.

Keywords: Activated carbon, Pyrolysis, Chemical Activation, Polyvinyl chloride, Optimization and Adsorption.

1. INTRODUCTION

Activated carbons (AC) are carbon-based materials that are synthesized via the oxidation of the carbon atoms that are found on both the inner and outer surfaces. They are usually prepared by the pyrolysis of materials containing a high percentage of carbon and low content of inorganic substances. This is followed by activation either by physical or chemical means. The activation of the carbonized products helps to oxidize the pores of the carbon and further develop their internal pore structures. Activated carbon are often characterized by large surface areas, highly-developed porosity, and tunable functional groups (Bansode *et al*., 2003, Zongxuam *et al*., 2003). The choice of precursors for the preparation of activated carbon depends on factors such as cost, availability and renewability of the material, amount of nutrient, and organic content of the material. In a bid to reduce the production cost, effort has been made by researchers all over the world towards utilizing renewable and relatively cheaper precursors. Such precursors include wood, agricultural byproducts (Wang *et al*., 2007), coal, synthetic resins, forest and industrial wastes (Cunliffe and Williams,1999, Lua and Yang, 2005, Ademiluyi *et al*., 2009).

However, previous studies have mainly focused on the preparation of the activated carbon from agricultural byproducts and forest wastes as an alternative for the commercial activated carbon (Buasri *et al*., 2013). Examples of such byproducts/wastes are plywood and chipboard wastes, grain sorghum (Diao *et al*., 2002), molasses (Legrouri *et al*., 2005), coconut shells (Radhika and Palanivelu, 2006), waste apricot (Basar, 2006), rubber wood sawdust (Prakash Kumar *et al*., 2006), oil palm fiber (Tan *et al*., 2007),, sugar beet bagasse (Onal *et al*., 2007), bamboo, rattan sawdust (Hameed *et al*., 2007).

The process of producing activated carbon involves two steps (Baker *et al*., 1992). The first step involves the carbonization of raw carbonaceous materials in an inert atmosphere. In this case, the carbon-containing materials are pyrolysed under inert conditions at temperatures ranging from 600 - 900 °C. The second step involves the activation of the carbon product. The carbonized material undergoes further treatment in order to enhance the porosity and adsorption performance for commercial application (Girgis *et al*., 2002). Activation could either be by chemical or physical means (Marsh and Rodríguez-Reinoso, 2006a; Inamullah *et al*., 2008).

Physical activation involves conversion of the precursor or carbonized carbon into activated carbons using gases or oxidizing atmospheres, and the activation temperature range of 600–1200 °C (Inamullah *et al*., 2008). Chemical activation involves the impregnation of the precursor raw material with some chemicals prior to carbonization, which may be typically an acid, a strong

base, or a salt. Impregnation dehydrates the carbon skeleton, thus, influencing the pyrolytic decomposition of the raw material, and it swells the interior of the botanic structure, leading to a porous structure. After impregnation, the raw material is then carbonized in under inert conditions. Chemical activation results in a more porous structure and a higher density carbon (Paraskeva *et al*., 2008). Generally, there is a preference for chemical activation over physical activation because a short residence time and a lower temperature is required for activation (Marsh and Rodríguez-Reinoso, 2006b; Mendez *et al*., 2006).

The use of polymeric wastes as precursors for activated carbon is currently being investigated by researchers and efforts are still being made to establish the feasibility of such studies (Lian *et* al., 2011). These wastes are commonly seen in waste bins and refuse dumps and are not easily degradable, thus, constituting serious environmental pollution. Hence, there is a dire need to get rid of them in an environmentally friendly manner. Specifically, the suitability of polyvinyl chloride (PVC) as a precursor in the synthesis of AC has rarely been documented This makes this area of research appears promising and is also aimed at achieving an alternative for the commercial activated carbon.

The objectives of this research are to produce AC from post-consumer PVC wastes using pyrolysis and chemical activation, investigate the physico-chemical properties of the produced carbons, optimize the processes involved, and validate the design model. Subsequently, the carbon produced under optimized conditions will be used to remove manganese, chromium, and cobalt ions from simulated water solutions and the adsorption and kinetics studies will be investigated.

2. EXPERIMENTAL METHODS

2.1. Materials and Samples Preparation

PVC wastes (precursor waste) were obtained from various construction sites in Ile-Ife, Osun State, Nigeria. The precursor wastes PW were washed properly with water and dried at room temperature for a period of 24 hrs. PW were crushed mechanically with a milling machine, and subsequently sieved using a screen mesh in order to obtain smaller particles with increased surface area for efficient chemical activation

2.2. Design of Experiment

The study was designed using Design Expert software package, version 10.0.1 (Stat-Ease Inc., Minneapolis, MN, USA). This is used in the determination of the coefficients of the polynomial model of the responses, the model equations, and their statistical significance. Table 1 shows the selected range of concentration of the chemical activating agents; 0.5 – 2.0 M (Al-Othman *et al*., 2011), carbonization temperature; 400 – 500 °C (Ademiluyi *et al*., 2009) and time; 45 – 60 min (Gonsalvesh *et al*., 2016). These factors were employed using the central composite design (CCD) in the design expert software and (nineteen) 19 random experimental runs were generated. These runs include eight (8) factorial points, six (6) axial points and five (5) center points.

Table 1: Selected Factor Levels for the Production of AC

Factors	Symbols	Unit	Level	
			Low	High
Concentration	A	mol/L	0.50	2.00
Temperature	B	°C	400	500
Time	C	min	45.00	60.00

2.3. RSM Statistical and Data Analysis

The responses selected were physicochemical properties (yield, moisture content, apparent density, iodine value), and adsorption performance; which was measured as a function of percentage removal of the inorganic ions (Mn^{7+}, Cr^{6+}, Co^{2+}) by the activated carbon from simulated water solution. The physicochemical tests were evaluated using standard methods and were used for the optimization of AC production. The quality of fit of the model was determined using analysis of variance (ANOVA) and test of significance.

The model response is represented by a quadratic fit as seen in equation 1:

$$Y = b_o + \sum_{i=1}^{k} b_i X_i + (\sum_{i=1}^{k} b_{ii} X_i)^2 + \sum_{i=1}^{k-1} . \sum_{j=i+1}^{k} . b_{ij} X_i X_j + e \quad (1)$$

Where: Y represents the predicted response factor, b_o denotes the value of intercept, b_i (i= 1, 2, ..., k) represents the first order linear model coefficient, b_{ij} shows the effect of the interaction coefficients, b_{ii} is the quadratic coefficients, X_i and X_j are the coded value of the process variables, and e represents the random error.

2.4. Pyrolysis and Chemical Activation

The chemical activating agents employed in this work are potassium hydroxide (KOH) and hydrogen tetraoxosulphate (VI) acid (H2SO4) at different concentrations as obtained by the design of experiment. Prior to pyrolysis, the prepared precursor wastes were activated with the corresponding activation agents at their respective selected factors. Pyrolysis was done in a reactor under a flow of nitrogen gas at the different corresponding temperatures and time. The samples (carbonized char) were removed from the reactor, crushed, and rinsed with distilled water. Selected conditions for the reaction were concentration (mol/L): A, temperature (oC): B and time (min): C. The chemically activated products were crushed and washed repeatedly with distilled water so as to get rid of residual inorganic matter and excess activating agent that may be present. Subsequently, they were dried and appropriately stored in a clean and closed container for further analysis.

2.5. Characterization of the AC

The percentage yield of activated carbon was determined using the procedure adopted by AlOthman *et al*., (2011). The dry weight of the pyrolysed product was determined with equation 2.

$$Yield\ (\%) = \frac{W_c}{W_o} \times 100 \quad (2)$$

W_c (g) is the dry weight of the AC and W_o (g) is the dry weight of PW.

The moisture content was determined according to standard procedure (ASTM D2867 -09). The bulk density of each AC sample was obtained using the method adopted by Al-Qodah and Shawabkah (2009) using a graduated measuring cylinder. The iodine values were determined according to ASTM standard method (ASTM D4607-14). All parameters were determined in triplicates and the average values recorded.

2.6. Determination of Adsorption Performance of AC

Simulated water solution was obtained by separately preparing 50 ppm of $KMnO_4$, 50 ppm of $K_2Cr_2O_7$ and 100 ppm of $CoCl_2$ in 1 L volumetric flask using distilled water. About 0.25 g was

put in 50 mL of the $KMnO_4$ solution and the resulting solution was agitated using the rotary shaker at 150 rpm for 120 min. Subsequently, the solution was filtered using Whatman No.1 (18.5 cm) filter paper, and the filtrate absorbance was determined using UV-Visible spectrophotometer at s specific wavelength 545.5 nm. The procedure was repeated for both K2Cr2O7 and CoCl2 simulated water solutions at 431 nm and 351 nm respectively. A standard calibration curve was obtained for each ion. The absorbance obtained was used to obtain the remaining concentration (Cf) of the adsorbate in each case by means of the calibration curve using Beer-Lambert law as expressed in equation 3:

$$\%\ removal = \frac{C_0 - C_f}{C_0}\ x\ 100 \quad (3)$$

Where C_o and C_f represents the initial and final concentrations (ppm) of the adsorbate in solution respectively.

2.7. Optimization of AC and Model Validation

Optimization for the production of AC was carried out by setting yield and bulk density in a range, moisture content and ash content were set to be minimum, and iodine value and adsorption performance were set to be maximum. Each of these precursors both have acid (H_2SO_4) and base (KOH) optimized AC.

The model was validated by repeating the experimental procedure for both pyrolysis and chemical activation step at the optimized factor levels for concentration, temperature, and time. The physicochemical properties of the optimized AC were investigated and was then characterized with Fourier Transform Infrared Spectroscopy (FT-IR).

The error was calculated with equation 4.

$$Error = \frac{Predicted - Actual}{Actual}\ X\ 100 \quad (4)$$

2.8. Optimization of Acid-Activated and Base-Activated Carbon Using UltraViolet Spectrophotometer (UV) Analysis

The AC with the best adsorption capacity between acid-activated and base-activated AC was determined. In this case, a simulated water mixture was prepared using 0.1 g of the inorganic ions in 1 Litre of distilled water. About 0.25 (g) of AC was put in 50 mL of the waste water mixture and was agitated with the rotary shaker at 150 revolution per minute (rpm) for a period of 120 min. This is followed by filtration and the Atomic Absorption Spectrophotometer (AAS) was used to analyse the filtrate in order to know the equilibrium concentrations of the respective ions presents in the solution.

Scanning Electron Microscopy (SEM) analysis was performed on the AC with the higher adsorption performance.

2.9. Adsorption and Kinetic Studies

This study was carried out for the uptake of manganese ions (Mn^{7+}) from aqueous solution unto AC produced under optimized reaction conditions at pH 6.5, different adsorbent dosage ranging from 0.25 – 1.00 g, different adsorbate concentrations ranging from 50, 75, 100, and 125 mg/L, all occurring at a constant agitation rate of 150 rpm. The isotherm data was analyzed and fitted to four different models: Langmuir, Freundlich, Temkin, and Dubnin-Radushkevich isotherms.

Langmuir isotherm: According to Dada *et al*., (2012), the Langmuir equation establishes the relationship between the adsorbate concntaration and the number of surface-active sites that is being adsorbed as expressed in equation 5.

$$q_e = \frac{q_m K_L C_e}{1 + K_L C_e} \quad (5)$$

Where q_e represents the equilibrium adsorption capacity (mg/g), C_e represents the equilibrium concentration of the adsorbate in solution (mg/L), k_L is the constant that relates to the free energy of adsorption (L/mg), and q_m denotes the maximum adsorption capacity (mg/g).

Equation 5 is rearranged in linear form to give equation 6:

$$\frac{C_e}{q_e} = \frac{1}{K_L q_m} + \frac{1}{q_m} C_e \quad (6)$$

A graphical illustration showing $\frac{C_e}{q_e}$ against C_e will give a straight line having a slope $\frac{1}{q_m}$ and intercept of $\frac{1}{K_L q_m}$.

Freundlich isotherm: This shows the relationship occurring between the amount of adsorbate adsorbed per unit mass of adsorbent (Anirudhan and Ramachandran, 2014). It is expressed by equation 7:

$$qe = K_f C_e^{\frac{1}{n}} \quad (7)$$

Linearizing equation 7 gives equation 8:

$$\log qe = \frac{1}{n} \log Ce + \log Kf \quad (8)$$

Where K_f is the Freundlich constants representing the adsorption capacity of the carbon, n represents the adsorption intensity which is a function of the system's characteristics.

Temkin isotherm: Temkin isotherm explains the molecular interaction within the adsorbed particles and adsorbent surface. It also explains the extent of heterogeneity of the adsorbent surface and that there is a uniform distribution of binding energy in the course of adsorption (Foo and Hameed, 2010). This relationship is expressed in equations 9, 10, and 11.

$$q_e = \frac{RT}{b} \ln(AC_e) \quad (9)$$

$$q_e = \frac{RT}{b} \ln A + \frac{RT}{b} \log C_e \quad (10)$$

$$q_e = B \ln A + B \ln C_e \quad (11)$$

A and B represents the Temkin isotherm constants, $B = \frac{RT}{b}$ which denotes the molecular interaction parameter, b relates to the heat of adsorption, T (K) is the absolute temperature, and R is the ideal gas constant (8314 $Jmol^{-1}\ K^{-1}$).

Dubnin- Radushkevich (D-R) model: This model adapts the earlier Polanyi potential theory of adsorption and is developed with respect to the postulation that adsorption in micropores occurs by filling of pores and not by a layer-by-layer film formation in the pore walls (Dada *et al*., 2012). It is often used to estimate the characteristic porosity of AC. The D-R isotherm equation is expressed by equation 12:

$$q_e = q_m e^{-\beta \varepsilon^2} \quad (12)$$

Simplifying gives:

$$\ln q_e = \ln q_m - \beta \varepsilon^2 \quad (13)$$

Where β is the free sorption energy per mole of the adsorbate as it moves to the surface of AC from an infinite distance within the solution ($KJ^2 mol^2$), ε is the polanyi potential ($Jmol^{-1}$), and q_m denotes the maximum adsorption capacity.

Equation (13) can be re-expressed by equation 14:

$$\varepsilon = RT \ln\left(1 + \frac{1}{C_e}\right) \quad (14)$$

Where R is the universal gas constant, T is the absolute temperature in kelvin, and C_e is the equilibrium concentration of the adsorbate in solution.

Kinetic Studies: This is the study of time dependence on the process of adsorption on solid surface as well as the determination of the adsorption mechanism. This helps to determine the adsorption process in industrial systems. In solid-liquid adsorption process, the kinetic helps in describing the rate of solute uptake which is usually a function of the residence time. The kinetic study of metal ions on adsorbent is usually done using pseudo-first order, pseudo-second order, and intraparticle diffusion models (Ho, 2006).

Pseudo-first order model: According to Ho, (2006), it is often expressed as:

$$\frac{dq}{dt} = k_1(q_e - q_t) \quad (15)$$

Where q_t is the adsorption capacity at any time t (mg/g) and k_1 is the pseudo first order rate constant (1/min). Integrating equation 15 and applying appropriate boundary conditions (at t = 0, qt = 0; and at t = t, qt = qt) gives:

$$\ln (q_e - q_t) = \ln q_t - k_1 t \quad (16)$$

Pseudo-second order model: The differential form is expressed by equation 17:

$$\frac{dq_t}{dt} = k_2 (q_e - q_t)^2 \quad (17)$$

Upon integration of equation 17, and then applying boundary conditions leads to equation 18:

$$\frac{t}{q_t} = \frac{1}{k_2 q_e^2} + \frac{1}{q_e} t \quad (18)$$

$$\frac{t}{q_t} = \frac{1}{h} + \frac{1}{q_e} t \quad (19)$$

Where $h = \frac{1}{k_2 q_e^2}$ ($mgg^{-1}min^{-1}$) is defined as the initial adsorption rate as $t \rightarrow 0$ and k_2 is the pseudo–second order rate constant (g/mg.min).

Intraparticle diffusion model: One major assumption associated with this model is that the rate-controlling step is the process involving film diffusion. The amount adsorbed at time t is directly proportional to the square root of the time of contact. This is expressed in equation 20:

$$q_t = k_{diff} t^{\frac{1}{2}} + C \quad (20)$$

Where q_t represents the amount of adsorbate at time t and K_{diff} ($mgg^{-1}min^{-1}$) is the intraparticle diffusion constant. The intercept C provides information about the thickness of the boundary layer. Higher values of the intercept lead to stronger effect of the boundary layer.

The characteristics parameters for the isotherms and models, together with their respective correlation coefficients were evaluated.

3. RESULTS AND DISCUSSION

3.1. Carbonization

The activated carbons produced from acid-activated and base-activated PVC wastes were designated PVC-H_2SO_4, and PVC-KOH respectively. The results obtained from the responses, physico-chemical tests and adsorption uptake of the different AC synthesized from the chemical activation and carbonization procedure are shown in Tables 2 and 3 for both acid- and base-activated precursors (*i.e.* PVC-H_2SO_4 and PVC-KOH) respectively. The effects of the model parameters on the responses and physico-chemical properties are discussed in subsequent sections.

Table 2: Effects of Concentration (mol/l), Temperature (°C), and Time (min) Against the Responses and Physico-chemical properties Obtained for PVC-H_2SO_4

Runs	Model Parameters			Responses						
	Conc. (mol/L)	Temp. (°C)	Time (min)	Activated Yield (%)	Moisture content (%)	Bulk density (g/cm^3)	Iodine value (mg/g)	%Mn^{7+} removal	% Cr^{6+} removal	% Co^{2+} removal
1	1.25	450	39.89	81.11	11.01	0.65	501.5	86.64	76.11	88.59
2	2.00	500	60.00	74.23	9.11	0.625	419.21	91.53	81.75	93.53
3	0.50	400	60.00	77.24	8.91	0.615	485.21	89.95	80.76	90.05
4	0.50	400	45.00	81.42	9.75	0.638	492.18	92.11	77.18	91.35
5	1.25	534.09	52.50	72.13	10.12	0.562	502.65	91.22	82.06	94.07
6	2.00	500	45.00	78.11	9.92	0.651	398.2	90.54	80.28	93.24
7	1.25	450	52.50	75.12	12.91	0.573	522.33	90.63	81.52	93.08
8	1.25	450	52.50	75.12	12.91	0.573	522.33	90.63	81.52	93.08
9	1.25	450	52.50	75.12	12.91	0.573	522.33	90.63	81.52	93.08
10	2.51	450	52.50	76.32	15.09	0.615	447.54	90.63	81.52	93.08
11	1.25	365.91	52.50	85.86	13.11	0.633	343.78	86.11	76.82	88.11
12	2.00	400	45.00	79.44	11.12	0.625	384.6	88.54	76.19	89.06
13	1.25	450	65.11	70.12	7.85	0.555	396.58	91.22	81.98	90.92
14	0.50	500	45.00	76.11	8.14	0.629	458.24	93.17	79.91	94.02
15	0.50	500	60.00	71.46	7.98	0.615	502.15	93.17	79.91	94.02
16	0.00	450	52.50	74.78	9.59	0.516	352.15	87.56	78.19	88.02
17	1.25	450	52.50	75.12	12.91	0.573	522.33	85.11	75.91	87.92
18	2.00	400	60.00	76.14	10.78	0.631	401.2	89.01	79.11	89.98
19	1.25	450	52.50	75.12	12.91	0.573	522.33	90.63	81.52	93.08

Table 3: Effects of Concentration (mol/l), Temperature (°C), and Time (min) Against the Responses and Physico-chemical properties Obtained for PVC-KOH

Runs	Model Parameters			Responses						
	Conc. (mol/L)	Temp. (°C)	Time (min)	Activated Yield (%)	Moisture content (%)	Bulk density (g/cm^3)	Iodine value (mg/g)	%Mn^{7+} removal	% Cr^{6+} removal	% Co^{2+} removal
1	1.25	450	39.89	82.11	10.95	0.541	643.15	91.99	71.02	94.89
2	1.25	450	52.50	77.11	12.07	0.565	740.84	91.82	70.74	94.05
3	0.00	450	52.50	77.12	9.21	0.642	611.20	91.98	70.65	94.02
4	2.00	400	60.00	79.42	10.51	0.612	502.33	87.02	74.99	88.98
5	1.25	450	65.11	72.23	7.05	0.617	613.84	92.81	70.11	94.68
6	0.50	400	60.00	79.19	8.14	0.502	647.74	86.89	74.84	88.64
7	0.50	500	45.00	80.01	7.81	0.598	695.12	90.18	61.65	91.04
8	0.50	400	45.00	81.21	9.61	0.565	740.84	91.82	70.74	94.05
9	1.25	450	52.50	77.35	12.01	0.629	601.42	88.95	69.01	90.87
10	2.51	450	52.50	78.79	14.81	0.565	740.84	91.82	70.74	94.05
11	2.00	500	60.00	76.12	8.95	0.629	634.53	92.85	71.88	92.10
12	1.25	365.91	52.50	85.86	12.95	0.615	598.20	89.18	73.21	90.11
13	2.00	400	45.00	81.25	10.99	0.565	740.84	91.82	70.74	94.05
14	0.50	500	60.00	74.66	7.52	0.551	701.58	92.11	71.01	94.98
15	1.25	534.09	52.50	75.21	9.86	0.609	634.53	92.85	71.88	92.10
16	2.00	500	45.00	80.61	9.71	0.618	647.18	94.62	73.11	92.01
17	1.25	450	52.50	77.11	12.11	0.612	702.15	87.18	64.22	89.11
18	1.25	450	52.50	77.11	12.11	0.603	704.18	95.11	76.81	97.11
19	1.25	450	52.50	77.11	12.11	0.565	740.84	91.82	70.74	94.05

3.2. Effects of Concentration, Temperature, and Time on the Yield of AC

The results of test of variance for every regression coefficient for both PVC-H_2SO_4 and PVC-KOH revealed the p-values of some model terms to be significant, ($p < 0.05$). The model linear terms (A, B, C) and quadratic terms (B^2 and C^2) for both PVC- H_2SO_4 and PVC-KOH were all less than 0.05 which implies that they are remarkably significant model terms at 95% confidence level; thus, the model proved adequate in representing the relationship that exists among the selected model factors of concentration, temperature and time. However, the model terms A^2, AB, and AC were not significant because their p-values were greater than 0.05.

It was also observed that temperature and time are the most significant model term that best predicts the yield of activated carbon via pyrolysis due to their respective higher F-value and lower P-value. This is in consonance with previous work done by Betiku and Adepoju (2013) where it was reported that for any model term, a very high F-value and a low P-value denotes the high significance of the model.

The overall model has p-values of 0.0011 and 0.0015, and F-values of 9.80 and 9.15 respectively which adequately proved the significance of the model on yield as a response. The values obtained has a low standard deviation and high "R-Squared (R^2)" values which indicates the good fit of the model. Betiku and Adepoju (2013) reported that a for a good fit of a model, the R^2 value should have a minimum value of 0.80. Their respective R^2 values of 0.9074 and 0.8929 is an indication that the sample variation of 90.74 % and 89.29 % for the production of the AC is associated to the independent factors (concentration, temperature, and time) and only 9.26 % and 10.71 % respectively of the total variation was not represented by the model.

The results obtained were graphically presented in order to provide a visual observation of responsive values and to examine the relationship between parameter levels. The 3D surface plot representing the interactive effect of temperature and time on AC yields while keeping the concentration constant are shown in Figure 1a and 1b.

From Figures 1a and 1b, it was observed that the yield value was significantly dependent on both the pyrolysis temperature and activation time. As temperature increases, the yield decreases. This is because an increase in carbonization temperature accelerates both elimination and dehydration reactions; thus, leading to an increase in the release of volatile materials. As both pyrolysis temperature and activation time increases, the % yield decreases as observed in Figure 1. This agrees with the study done by Gonsalvesh *et* al., (2016) where it was reported that increasing the activation time from 30 to 120 min, led to a decrease in the AC yield produced from polystyrene (PS) precursor from 48 to 33 %.

For PVC-H_2SO_4, an optimum yield of 80 % was obtained at a temperature of around 450 °C and time of about 50 min while for PVC-KOH, an optimum yield of 80.70 % was obtained at 425 °C and 48 min. These values are relatively higher than those obtained by Qiao *et al.*,(2004) where a yield of 9 – 18 % of AC was reported to be gotten from a value resin PVC material. The low yield reported was assumed to be due to the steam activation process employed using a spinnable pitch. However, the AC obtained at lower temperatures and time may not have the desired quality in terms of porosity when compared with those obtained at higher temperatures and time.

Table 3 shows a summary of the test of significance and final equations expressed as a function of coded factors with respect to activated yield for the AC produced. The models were found to be significant. These equations can be used to predict the response for given factor levels and are also often used to identify and establish the relative impact of the factors. This is usually achieved by comparing factor coefficients. For instance, for PVC-H_2SO_4, the model term with the highest factor coefficient is B and has a value of -2.74. The negative sign indicates that the response yield is indirectly proportional to the model term B (temperature), while the value of 2.74 shows that the model term is the most significant that best predicts the model.

Table 3: A Summary of the Test of Significance and Final Equations in Terms of Coded Factors with Respect to Activated Yield for the AC Produced

Source of AC	Prob > F	Model Equations
PVC-H_2SO_4	0.0011 (significant)	+75.12 + 0.31*A -2.74 *B – 2.53*C + 0.98*AB + 0.21*AC – 0.13*BC + 0.14*A^2 + 1.36*B^2 + 0.16*C^2
PVC-KOH	0.0021 (significant)	+77.09 + 0.38*A – 2.02*B - 2.22*C + 0.22 *A*B + 0.13*AC – 0.75*BC + 0.39*A^2 + 1.30*B^2 + 0.11*C^2

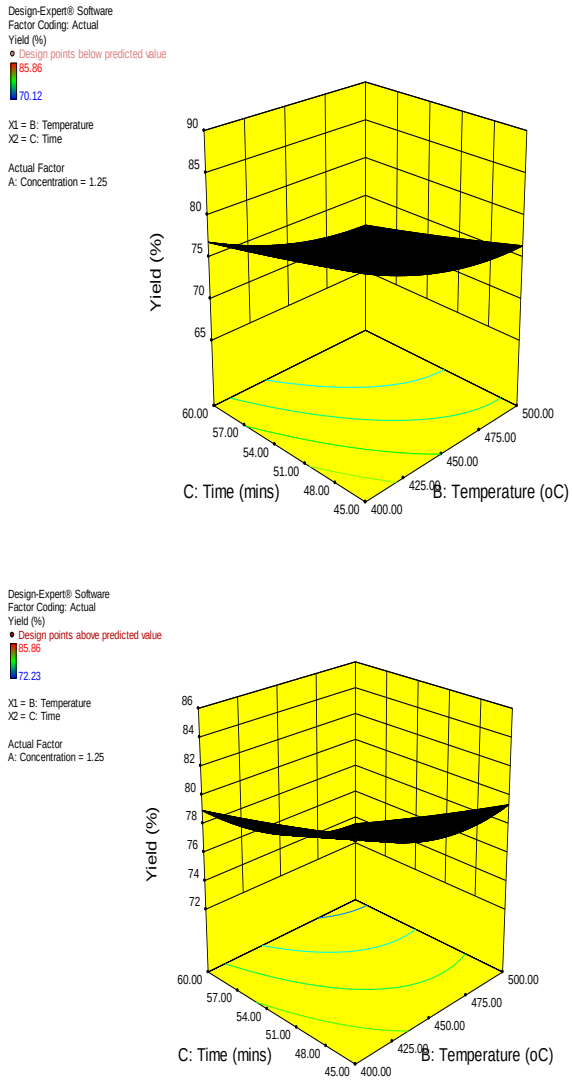

Figure 1: The 3D Surface Plot Showing the Interactive Effect of Temperature and Time on Activated Yield of (a) PVC-H_2SO_4 (b) PVC-KOH

3.3. Effects of Concentration, Temperature, and Time on Iodine Value of AC

The iodine values of AC produced are shown in Table 2. PVC-H_2SO_4 is similar in behavior to PVC-KOH with respect to the model terms. The linear term of B, and the quadratic terms A^2 and B^2 are quite significant due to their low p-values of less than 0.05. Moreover, the model F-value of 3.90 represents the significance of the model, and thus gives a good representation of the relationship among the factor levels. The values of coefficient of variation and adequate precision of 6.29 and 8.209 respectively fall within the acceptable limit, and thus represent a significance of the model. The obtained data best fit a quadratic model.

Figure 2 shows the interaction between concentration and temperature. Higher iodine values were obtained at concentrations near 1.0 M and temperature of around 470 °C. The iodine values of AC produced from PVC-KOH has an optimum value of 740.84 mg/g at conditions of 445 °C, 1.00 M, and 50 min. PVC-H_2SO_4 has an optimum value of 522 mg/g under conditions of 1.00 M, 445 °C, and 48.50 min.

At lower concentrations, the iodine value was relatively low due to insufficient quantity of activating agent to react with the carbonized carbon to efficiently open up the internal pore structures. However, at much higher concentrations and temperatures, the micropore structure of PVC-AC produced might have deteriorated due to excessive carbonization.

Moreover, the interactive effect between concentration and time shows that the iodine number increases as activation time increases. This deduction agrees with previous study carried out by Gonsalvesh *et al*., (2016) where the iodine adsorption capacity of AC produced from polystyrene (PS) precursor increased from 920 to 1000 mg/g as activation time gradually increases from a period of 30–120 min. It was also observed that an increase in carbonization temperature gave rise to higher iodine values for all AC samples until an optimum point was reached and is in agreement with results obtained by Gonsalvesh *et al*., (2016) whereby it was reported that at an activation time of 30 min, the iodine number of AC produced from polystyrene (PS) precursor continually increases from 650 to 970 mg/g as activation temperature rises from 750 to 900 °C and then decreases to 950 mg/g at 950 °C. This suggests that an optimum iodine value is always reached such that any further increase in temperature seems to be relatively insignificant.

Factor coefficients were compared to establish the impact of the factors and it was observed from the model equations of PVC-H_2SO_4 and PVC-KOH that the quadratic terms A^2 have higher coefficients of 38.07 and 33.98 respectively. This indicates that the quadratic term of concentration (A^2) is the most significant model term in iodine value determination of AC. Thus, the concentration of the activating agent used best predicts the iodine value.
The iodine values obtained are relatively higher than the values reported by Adibfar *et al*. (2014) and La´szlo´ *et al*. (2003). The latter reported an iodine value of 402 mg/g for polyethylene terephthalate (PET) while studying the effect of heat on certain synthetic carbon precursors. The higher value of iodine number of AC produced from PVC wastes is a function of the nature of the material, since these polymeric wastes have a higher percentage of carbon when compared to activated sludge. Higher values of iodine numbers indicate higher adsorption capacity.

3.4. Effects of Concentration, Temperature, and Time on Moisture Content and Bulk Density of AC

The model linear terms A, B, C, and the quadratic terms B^2 and C^2 are significant model terms for AC produced from PVC as observed in Table 4. Thus, all the reaction parameters are active determinants in the amount of moisture present in the AC.

Table 4: A Summary of the Test of Significance and Final Equations in Terms of Coded Factors with Respect to Moisture Content for the AC Produced

Source of AC	Prob > F	Model Equations
PVC-H2SO4	0.0011 (significant)	+12.97 + 1.13*A – 0.76*B – 0.55*C – 0.041*AB - 0.019*AC + 0.026*BC - 0.53*A2 - 0.79*B2 – 1.56*C2
PVC-KOH	0.0107 (significant)	+12.17 + 1.21*A – 0.77*B – 0.70*C – 0.053*AB + 0.065*AC + 0.11*BC – 0.37*A2 – 0.58*B2 – 1.43*C2

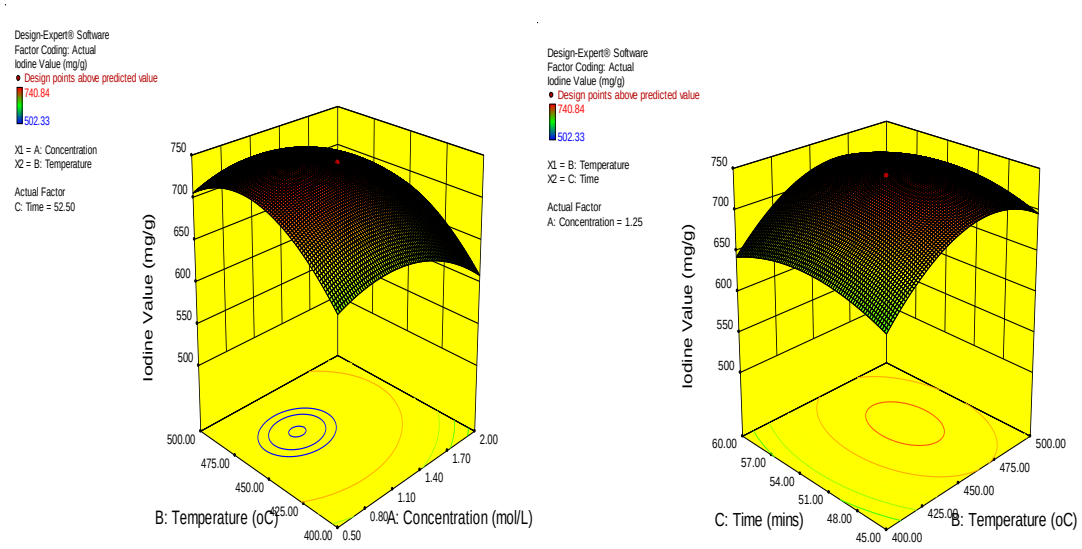

(a) *(b)*

Figure 2: 3D Surface Plot Showing the Interactive Effect of (a) Concentration with Temperature (b) Temperature with Time on Iodine Value of PVC-KOH

Figure 3 shows the 3D contour plot representing the interactive effect of concentration and temperature on the moisture content of AC obtained from PVC-H_2SO_4.

From Figure 3, the moisture content of the AC samples has values in the range of 7.85 – 15.09 % and was seen to increase as the concentration of H_2SO_4 increases. This is due to the polarity of the acid. However, the amount of moisture found in PVC-KOH has values within 7.05 – 14.81 %. The amount of moisture content present in the carbons was also found to decrease as temperature and time increases and this can be attributed to the continuous evaporation of volatile matter as the reaction progresses. The moisture content of KOH-activated carbons is generally higher than the H_2SO_4-activated carbons. This is in consonance with previous work done by Adibfar *et al.* (2014) where they reported that moisture content of AC produced from KOH-activated PET and H_2SO_4-activated PET were 6.7 % and 2.7 % respectively. These higher values of KOH-activated carbons are due to the high affinity of KOH for water absorption. However, it is desirable that an AC should be such that it has low moisture content.

The bulk densities of the AC produced have values in the range of 0.411 to 0.642 g/cm^3. The obtained values are however slightly higher than those reported by Adibfar *et al.* (2014) where values in the range of 0.20 – 0.33 g/cm^3 were observed for chemically activated samples using different chemical agents such as KOH, H_3PO_4, $ZnCl_2$, and H_2SO_4. These observed differences are an indication that bulk densities of carbon are strongly influenced by factors such as particle size distribution, method of treatment/activation, the type and concentration of the chemical activating agents. However, due to the "thickness" of the precursor waste of PVC, the model terms of concentration and time were found to be significant in the prediction of the model as regards bulk density.

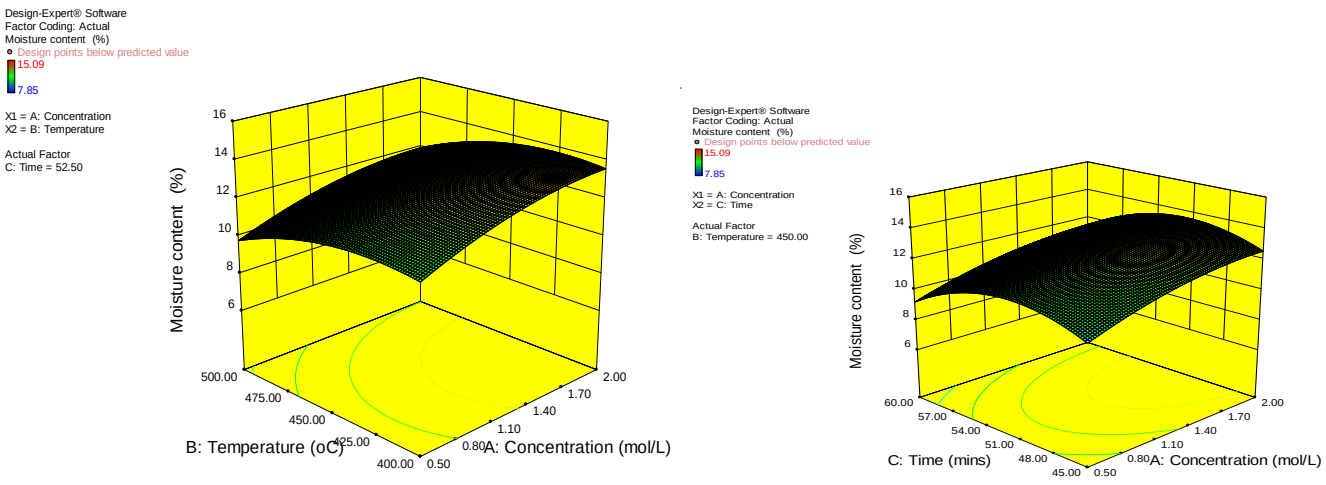

(a) *(b)*

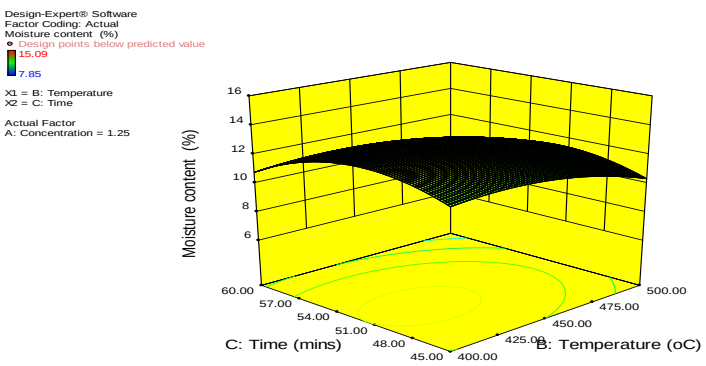

(c)

Figure 3: 3D Surface Plot Showing the Interactive Effect of (a) Concentration and Temperature (b) Concentration and Time (c) Temperature and Time on the Moisture Content of AC Produced from PVC- H_2SO_4

It was generally observed that the bulk density slightly increases as the concentration of the chemical activating agent increases as shown in Figure 4. This phenomenon is due to the higher moisture content found in higher concentrations of the AC. In other words, the higher the concentrations of KOH, the higher the moisture content of the produced carbons and the higher the bulk density. However, the optimum values of 0.651 and 0.642 g/cm^3 for PVC-H_2SO_4 and PVC-KOH respectively was reached after which a further increment in concentration of the activating agent does not affect the bulk density of the AC produced.

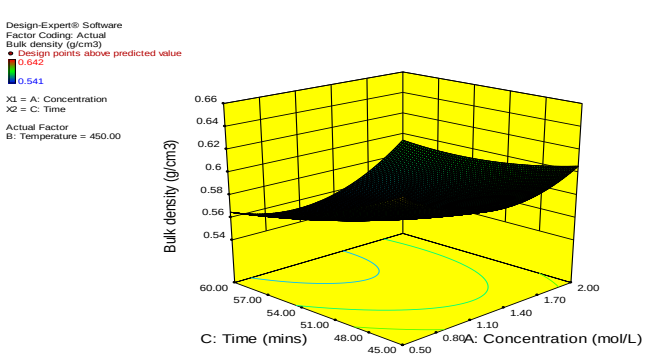

Figure 4: 3D Surface Plot Showing the Interactive Effect of Concentration and Time on Bulk Density of AC Produced from PVC-KOH

3.5. The Adsorption Performance of AC on Mn^{7+}, Co^{2+}, and Cr^{6+} solution

The investigation of the adsorption performance of the different activated carbons produced using simulated polluted water solution containing manganese, cobalt, and chromium ions shows that both PVC-H_2SO_4 and PVC-KOH have higher adsorption capacity for Mn^{7+} (85-95 %) and Co^{2+} (88-97 %) than Cr^{6+} (61-82 %). These values obtained are in reasonable agreement to those reported by Aji *et al.* (2015) where the adsorption performance of AC produced from groundnut shell was reported to have 84 % Manganese removal.

Moreover, a visual observation shows a drastic change in color from the initial purple state of manganese-simulated water solution to a colorless state at equilibrium. This is due to the removal of the ions from the aqueous solutions which is principally as a result of the reduction from its initial state of Mn^{7+} to Mn^{2+}. This strongly indicates that the AC produced has a high affinity for manganese ions and can be used for its removal in any adsorption system.

The equation of the reduction reaction is expressed in equation 21:

$$MnO_4^-(aq) + 8H^+(aq) + 5e^- \rightarrow Mn^{2+}(aq) + 4H_2O\ (l) \quad (21)$$

It was observed that AC obtained from these polyvinyl chloride wastes under moderate concentrations of 0.50 – 0.80 M, temperatures above 480 °C and activation time above 45.00 min have a higher adsorption performance. In other words, high carbonization temperatures, coupled with moderate concentrations of chemical activating agent and minimal activation time of 45 min helps to develop the pores of the carbon and makes it surface available for adsorption.

In the case of chromium removal, it was generally observed that PVC-H_2SO_4 has higher adsorption capacity (in the range of 75 - 82 %), than PVC-KOH (61-77 %). The different levels of the reaction parameters were responsible for the range in values. AC obtained at temperatures ›450 °C and concentrations ›1.25 M gives a higher adsorption rate for chromium removal. The adsorption capacities were found to increase with increasing carbonization temperatures. An increase in temperature widens the carbon pores, thus increases the porosity accessible to chromium ions. Specifically, reaction conditions of 2.0 M, 500 °C, and 60 min gives optimum adsorption rate for chromium with a percent removal of 81.75 and 74.99 for AC produced from PVC-H_2SO_4 and PVC-KOH respectively. Moreover, the physical change in color from yellow to very light yellow was also observed in the course of the reaction. This weak adsorption of chromium ions can be attributed to the inability of the AC to reduce Cr^{6+} to Cr^{3+}. The chemistry of reaction is represented in equation 22.

$$Cr_2O_7^{2+}(aq) + 14H^+(aq) + 6e^- \rightarrow 2Cr^{3+}(aq) + 7H_2O(l) \quad (22)$$

The performance evaluation of these activated carbons in the treatment of cobalt-containing simulated water was studied and similar observations were made when compared to manganese- and chromium-containing water solutions. Depending on the nature of the products, there was a gradual color change from the initial lilac solution to a pure colorless solution at equilibrium, thus implying complete removal of the ions from the mixture. PVC-H_2SO_4 with a maximum adsorption rate of 94 % occurs under the reaction conditions of 0.5 M, 500 °C and minimal activation time of 45 min, while PVC-KOH has an adsorption capacity greater than or equal to 94 % under minimum reaction conditions of 1.1 M, 475 °C, and 54 min.

The AC produced can be said to be highly suitable for the removal of some inorganic ions in aqueous systems.

Table 5 shows the optimization conditions and results employed in the validation of the model.

Table 5: Model Validation for Yield, Moisture Content, Bulk Density, Ash Content, Iodine Values, for the Production of AC

Source of AC	Optimized Reaction Conditions			Yield (%)			Moisture Content (%)			Bulk Density (g/cm^3)			Iodine Value (mg/g)		
	Conc. (mol/L)	Temp. (°C)	Time (mins)	Actual	Pred.	Error (%)	Actual	Pred.	Error (%)	Actual	Pred.	Error (%)	Actual	Pred.	Error (%)
PVC-H_2SO_4	0.50	500.00	46.46	73.86	75	1.54	8.35	9.19	9.14	0.5398	0.5969	9.57	457.25	467.93	2.28
PVC-KOH	0.50	500.00	55.35	73.28	75	2.29	7.97	8.84	9.84	0.5165	0.5619	8.08	699.22	709.15	1.40

3.6. FT-IR Results on the ACs

FT-IR analysis was done in order for identification of the functional groups present in the optimized AC obtained using the optimized reaction conditions obtained in Table 5. Figures 5 and 6 shows the IR spectra of both acid and base activated AC produced from PVC. The measurements were carried out over the range of 4000 – 650 cm^{-1}. The peaks shown in the FT-IR spectrum were attributed to different functional groups according to their corresponding wave numbers. The FT-IR analysis results obtained indicate only minor differences between both acid and base activated samples because they exhibit similar IR Spectroscopic features.

Generally, the spectra obtained for each AC samples show the presence of oxygen surface complexes in the form of carboxyls, phenols, alcohols, ketones, ethers, and aldehydes. This is due to the introduction of chemical activating agents on the carbon surface. The bands at 3429 – 3397 cm-1 represent strong broad bands associated with intramolecular hydrogen bonding attached to O-H groups. This is as a result of the absorption of molecules of water due to an O-H stretching mode of hydroxyl groups and adsorbed water. The band at 2120 cm-1 is attributed to the –CH stretching of a methylene group and is responsible for the interaction with the surface of the carbon. It may also belong to the stretching frequencies of C=C bond of the acetylene family (Attia et al., 2006), thus indicating the presence of carbon in the AC structure. It may also be attributed to presence of isocyanates (-N=C=S) in the carbon structure, and this may be as a result of the presence of fillers in the precursor polymer PVC.

The bands at 1891 cm^{-1} may be attributed to the stretching frequency of C=O group. In the region 1695 – 1645, aldehyde functional groups can be distinguished on the carbon surface (Misra *et* al., 2005) which has peaks at 1684, 1679, and 1654 cm^{-1}, and these may be caused by the intramolecular H-bond that may have been formed between the carbon surface and the chemical activating agents. This may also be due to the hydrogen-bonded OH group of alcohols and phenols (Park *et al*., 1997). Moreover, the bands at 1541 and 1507 cm^{-1} may be attributed with primary and secondary amides that may exist in the precursor polymeric material. The two peaks at 1101 and 1100 cm^{-1} yield the fingerprint of these carbons. These peaks may indicate the presence of silicon, and/or C-O stretching in alcohol, ether or hydroxyl groups (Attia *et al*., 2006). The peaks around 875 and 670 cm^{-1} indicates C-H out-of-plane bending.

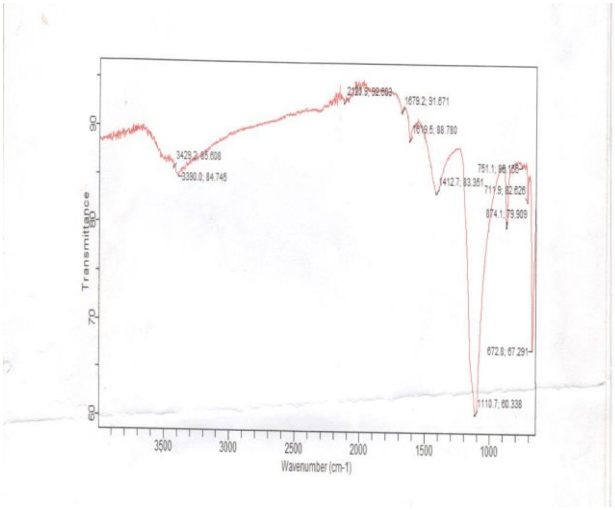

Figure 5: FT-IR Spectrum for AC from PVC-H_2SO_4

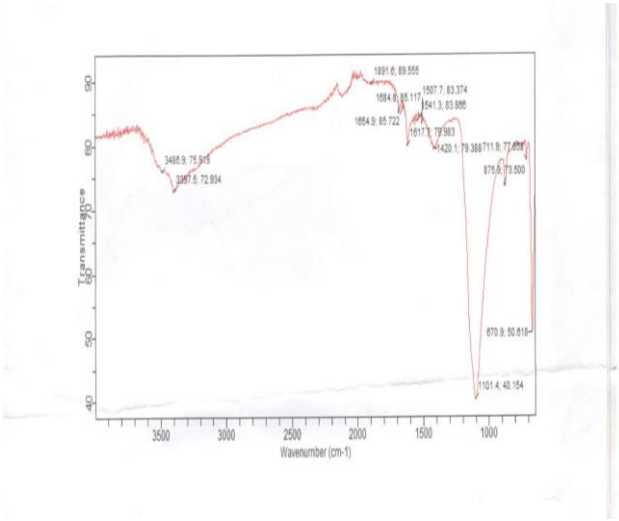

Figure 6: FT-IR Spectrum for AC from PVC-KOH

3.7. Optimization of Acid and Base Activated AC using AAS Analysis

The results obtained from the AAS analysis is shown in Table 6. It was observed that the adsorption capacities of the ACs are high in the removal of manganese and cobalt ions. It is however relatively low in the removal of chromium ions from aqueous solutions. This may be attributed to the nature of the polymeric materials to be able to reduce both manganese and cobalt ions from higher oxidation states to lower oxidation states.

Table 6: Table of results showing AAS Analysis for the Removal of Inorganic Ion by AC: pH= 6.5, adsorbent dosage: 0.25 g/ 50 mL adsorbate, Initial adsorbate concentration Co = 100 ppm each for Mn^{7+}, Cr^{6+}, and Co^{2+}.

	PVC- H_2SO_4			PVC- KOH		
	Mn^{7+}	Cr^{6+}	Co^{2+}	Mn^{7+}	Cr^{6+}	Co^{2+}
Co	100	100	100	100	100	100
Ce	0.245	45.979	0.299	0.244	45.474	0.282
Co-Ce	99.755	54.021	99.701	99.756	54.526	99.718
Adsorption Capacity	19.95	10.804	19.940	19.951	10.905	19.944
% Removal	99.76	54.02	99.70	99.76	54.53	99.72

On the other hand, the base-activated AC obtained from PVC wastes was found to have higher adsorption capacity than the acid-activated carbon. Based on these observations, it was concluded that the AC with the best adsorption capacity is the base-activated carbon.

The final appearance of the activated carbon produced is shown in Plate 1.

Plate 1: Synthesized AC produced from PVC under optimized conditions from PVC

3.8. SEM Analysis of the AC

SEM analysis was performed on the base-activated AC produced under the best operating conditions with a higher adsorption performance as obtained from the AAS results.

The effect of activation on porosity was investigated so as to observe the surface physical morphology and crystal structures of the derived activated carbons.

The SEM micrographs of AC produced from PVC under the optimized conditions of 0.50 M of KOH, carbonization temperature of 500 °C, and activation time of 55.35 min are shown in Figure 8. The images show the presence of holes, cave openings and pores on the surface of the carbon.

The external surface of the chemically activated carbons is rich with cavities and highly porous in nature causing an increase in the number of surface sites that is available for adsorption. The micrograph also shows the presence of wide pores as a result of chemical activation.

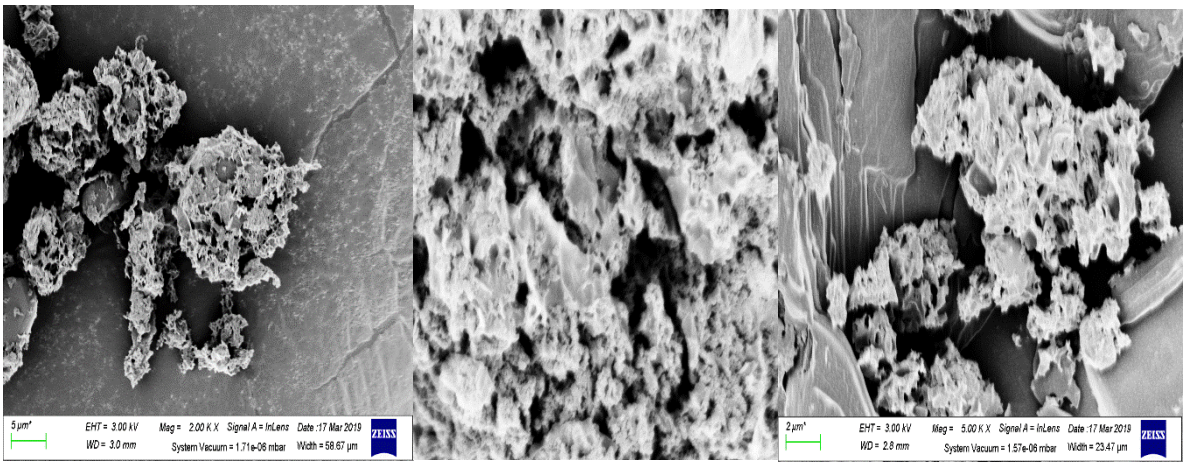

Figure 8: *SEM Images of Optimized AC produced from KOH-Activated PVC*

3.9. Adsorption Studies

The adsorption isotherm model parameters are shown in Table 7. It was observed that the maximum adsorption monolayer capacity of the Langmuir isotherm model (Q_L) decreases from 54.054 mg/g to 16.8634 mg/g as the adsorbent dosage is increased from 0.25 g to 1.00 g. This implies that as the mass of adsorbent increases, the capacity of the adsorbates to undergo physical adsorption on the surface of adsorbents at monolayer coverage decreases. However, this data does not fit the model adequately when a small adsorbent mass of 0.25 g was used as seen in the R-squared values of 0.793 and illustrated in Figure 9a. When higher amount of mass of adsorbent is used, the model fits almost perfectly. Also, the values of R_L indicate the type of adsorption involved in terms of favourability. At R_L= 0, there is irreversible adsorption; there is a favourabe adsorption when $0< R_L<1$; an unfavourable adsorption when $R_L>1$, and a linear adsorption at R_L=1. The values of R_L obtained are all less than one (1) but greater than zero (0) which indicates that the adsorption process is a favourable one. Furthermore, the high values of the Langmuir constant K_L indicates that the AC has a large surface area and pore volume; thus, a high adsorption capacity.

The Freundlich model fits the model better than the Langmuir isotherm due to its higher R-squared values as observed in Figure

9b. At an adsorbent dosage of 0.75 g, the Freudlich model fits almost perfectly (R^2= 0.999), thus, suggesting that an optimum amount of adsorbent mass is needed for the adsorption study. Moreover, values obtained for the adsorption intensity (1/n) and Freundlich adsorption capacity K_f obtained from this model suggest strongly that there is a relative distribution of energy during the adsorption process, adsorption occurs on heterogeneous surfaces, and that the interaction between manganese molecules are satisfactory at the different adsorbate concentrations of 50, 75, 100, and 125 ppm.

Table 7: Parameter Values for Each Isotherm Model

Adsorbent Dosage (PVC) (g)	Langmuir Isotherm Constants				Freundlich Isotherm Constants			Temkin Isotherm Constants			D-R Isotherm Constants		
	Q_{max} (mg/g)	K_L (L/mg)	R_L	R^2	n	K_F	R^2	A	B	R^2	$q_{m,D-R}$	E (KJ/mol)	R^2
0.25	54.0540	0.3544	0.0220	0.7930	2.7678	18.4884	0.8506	5.1733	10.6162	0.7579	37.6563	16.5576	0.7142
0.50	29.0698	1.6538	0.0048	0.9832	15.125	2.180	0.9317	7.8795	7.916	0.9807	25.1737	0.0214	0.9808
0.75	22.4719	3.2721	0.0024	0.9765	2.1363	18.5567	0.9990	31.2178	5.0017	0.9730	17.1397	22.2896	0.9507
1.00	16.8634	6.0510	0.0013	0.9323	2.1744	18.3865	0.9814	62.6150	3.6421	0.9291	13.5204	27.2991	0.9273

The Temkin isotherm takes into cognizance the interactions occurring between the manganese ions and AC. The Temkin model also fits the experimental data well (as shown in Figure 9c) due to high correlation coefficient, most especially when the mass of adsorbent was taken as 0.5 g and 0.75 g with R^2 values of 0.9807 and 0.9730 respectively.

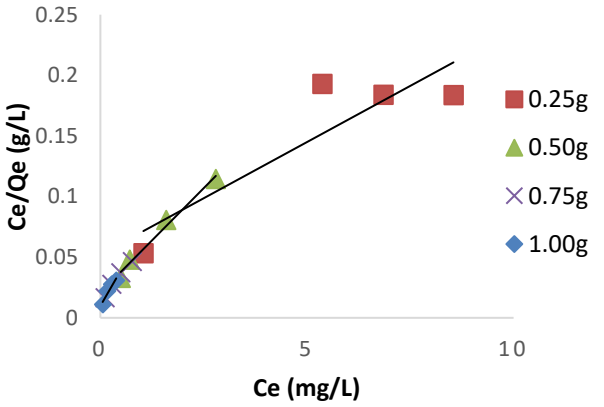

Figure 9a: Langmuir Adsorption Isotherm of AC Obtained from PVC-KOH under Optimized Reaction Conditions

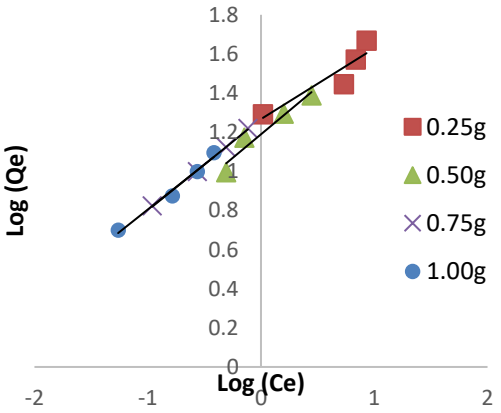

Figure 9b: Freundlich Adsorption Isotherms of AC Obtained from PVC-KOH under Optimized Reaction Conditions

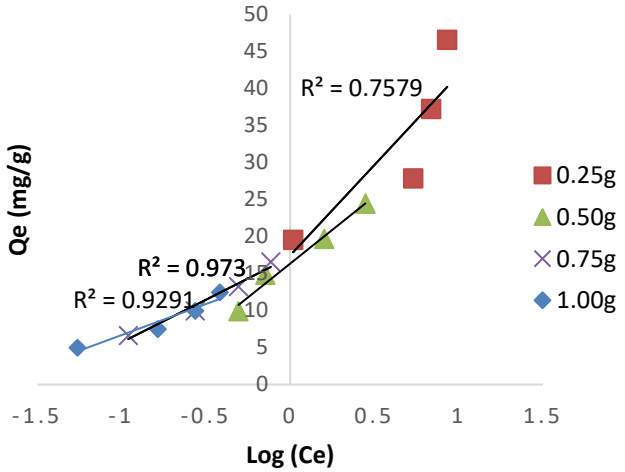

Figure 9c: Temkin Adsorption Isotherm of AC Obtained from PVC-KOH under Optimized Reaction Conditions

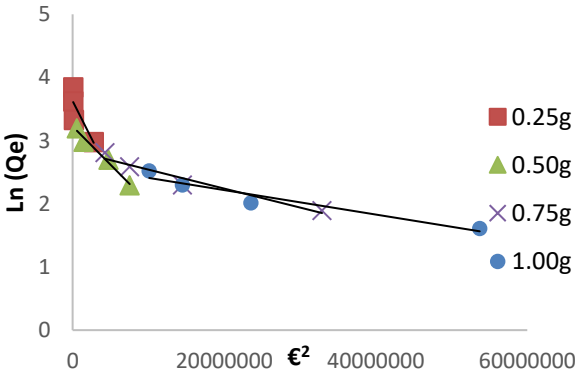

Figure 9d: D-R Adsorption Isotherms of AC Obtained from PVC-KOH under Optimized Reaction Conditions

These high values of R^2 confirms that the adsorption of manganese ion in the layer have a linear correlation with coverage due to carbon-manganese interactions and that the adsorption is accompanied by a uniform distribution of binding energies. However, the equilibrium data obtained at an adsorbent mass of 0.25 g does not fit into the model adequately. This similar observation was noticed in the Langmuir model.

The equilibrium data were tested with D-R model and values of the D-R monolayer capacity Qm (mg/g), the Polanyi potential €, and the mean energies of adsorption (E) which is a function of the sorption energies were obtained. The model also fits the data as shown in the Figure 9d.

Generally, the adsorption data was found to perfectly fit the Freundlich model at an adsorbent dosage of 0.75 g/100 mL of adsorbate.

3.10. Kinetic Studies

The kinetic studies of manganese ion adsorption onto AC obtained from PVC-KOH were investigated with the help of kinetic models in order to have a quantitative understanding of the sorption processes. This investigation was carried out at an adsorbent dosage of 0.75 g, pH 6.5, adsorbate concentration of 100 mg/L, and at an agitation rate of 150 rpm. The estimated coefficient of correlation R was applied in the determination of the most suitable kinetic model for manganese ion adsorption. The results obtained are shown in Table 8.

The pseudo-first order plot of PVC-KOH as represented in Figure 10a reveals that equilibrium is reached at a period between 60 – 75 min. From the plots, the kinetic rate constant of PVC-KOH was found to be 0.0891 min^{-1} and the correlation coefficients obtained to be 0.9911. This high value confirms the fact the pseudo-first-order model can be possibly applied to the sorption process.

On the other hand, the linearized form of the pseudo-second-order rate equation was used to estimate the parameters. A graph of t/Q_t against t gave a straight line as shown in Figure 10b. The slope of the plot was used to determine the kinetic rate constants K_2, while the intercepts obtained was used to estimate the kinetic parameters: equilibrium amounts of manganese ions (mg/g) Qe and the initial rate of adsorption (h) as t tends to zero. The correlation coefficient was obtained as 0.9988 which is relatively higher that obtained in the pseudo-first-order kinetics. Hence, this is a confirmation that the sorption of manganese ions onto activated carbon follows a pseudo-second-order kinetics.

Table 8: Table showing the Kinetic Rate Parameters and Estimated Corrrelation Coefficients for the Different Kinetic Models

Source of AC	Pseudo-first-order Constants			Pseudo-second-order Constants				Intraparticle diffusion Constant	
	K_1 (min^{-1})	Qe (mg/g)	R^2	K_2 (min^{-1})	Qe (mg/g)	h(mg/g.min)	R^2	Kp ($g/mg.min^{1/2}$)	R^2
PVC-KOH	0.089	38.7525	0.9911	0.0178	10.4493	1.94363	0.9988	0.65	0.9886

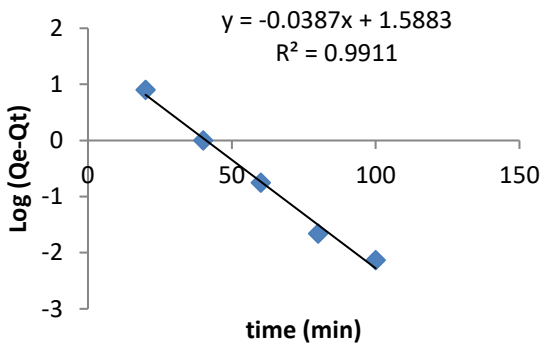

Figure 10a: The Pseudo-First-Order Kinetic of Mn^{7+} adsorption on AC obtained from PVC-KOH: pH6.5, adsorbent dosage 0.75 g/100 mL of adsorbate concentration.

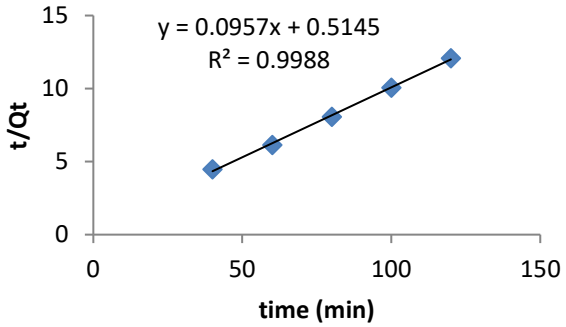

Figure 10b: The Pseudo-Second-Order Kinetic of Mn^{7+} adsorption on AC obtained from PVC-KOH: pH 6.5, adsorbent dosage 0.75 g/100 mL of adsorbate concentration.

The intraparticle diffusion model helps to identify the diffusion mechanisms and participation of the different processes involved in the sorption of manganese ions by AC. In this model, the rate of intraparticle diffusion as a function of $t^{1/2}$ is presented in Figure 11. The plot shows the intraparticle diffusion model at an adsorbate concentration of 100 mg/L, and adsorbent dosage of 0.75 g.

It was observed from this plot that there is multilinearity, thus indicating that the mechanism of diffusion involves more than one step. The first step is the surface adsorption occurring at the external site. This stage is otherwise known as the instantaneous adsorption stage and is completed before 20 min. The second step is the adsorption stage, it occurs gradually from 20 to 75 min and is the region where intraparticle diffusion is rate-controlled. The constant Kp ($mg/g.min^{1/2}$) is obtained from the slope of the line in the second stage. The third or final stage represents the equilibrium stage where the diffusion that occurs within the molecules begins to reduce because of the presence of low adsorbate concentrations in the solutions. This equilibrium adsorption stage starts after about 75 min. The manganese ions are transported gradually through intraparticle diffusion into the AC particles and subsequently retained in the pores.

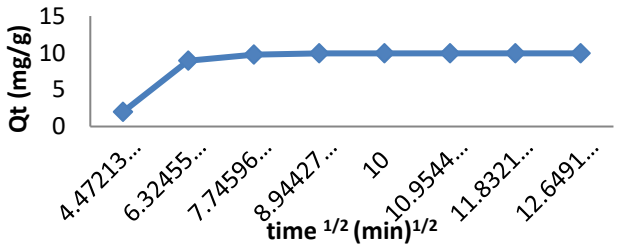

Figure 11: Intraparticle Diffusion plot for Mn^{7+} Adsorbed onto PVC-KOH at initial concentration Co = 100mg/L; pH = 6.5, room temperature, adsorbent dosage = 0.75 g

4. CONCLUSION

The feasibility of producing activated carbon from post-consumer polyvinyl chloride waste was investigated. The effects of the model parameters were studied and used in the optimization studies. Based on the findings of this research, it can be concluded that post-consumer PVC wastes are excellent substitutes for use as an alternative precursor for the production of low-cost activated carbon. AC produced from these wastes are very suitable for use as adsorbents in the removal of inorganic ions from aqueous solutions. The process of chemical activation leads to an increase in porosity of the carbons.

Moreover, the optimization studies proved the model parameters and overall model to be significant with respect to the responses of the model. An optimized concentration of 0.50 M and optimized temperature of 500 °C were statistically obtained for both PVC-H_2SO_4 and PVC-KOH while the optimized time was

46.46 and 55.35 min respectively. FT-IR analysis shows the presence of oxygen-surface complexes such as the carbonyls, aldehydes, and O-H groups on the surface of the AC which is as a result of the introduction of chemical activating agents. The SEM results showed that all the AC produced from the precursor wastes have a large surface area and pore volumes which makes them very suitable for use as adsorbents.

Furthermore, based on the overall adsorption rate using the percentage adsorption of inorganic ions (Mn^{7+}, Cr^{6+}, Co^{2+}) from aqueous solutions as the performance indicator, it can also be concluded that both acid-activated and base-activated carbons are suitable for use as adsorbents due to their high adsorptive capacities.

REFERENCES

Ademiluyi, F. T., Amadi, S. A., and Amakama,N. J., "Adsorption and Treatment of Organic Contaminants using Activated Carbon from Waste Nigerian Bamboo". J. Appl. Sci. Environ. Manage.13(3): 39-40, 2009.

Adibfar, M., Kaghazchi, T., Asasian, N., and Soleimani, M., "Conversion of Poly(Ethylene Terephthalate) Waste into Activated Carbon: Chemical Activation and Characterization". Chemical Engineering Technoogy, 37(6):979–986, 2014.

Aji, M.M., Gutti, B., and Highina, B. K., "Production and Characterization of Activated Carbon from Groundnut Shell Sourced in Maiduguri". Columbia J. Life Sci. 17(1): 18-24, 2015.

Al-Qodah, Z. and Shawabkah, R. "Production and Characterization of Granular Activated Carbon from Activated Sludge". Brazilian Journal of Chemical Engineering. 26(1): 127 – 136, 2009.

AlOthman, Z. A., Habila, M.A., and Ali, R., "Preparation of Activated Carbon Using the Copyrolysis of Agricultural and Municipal Solid Wastes at a Low Carbonization Temperature", International Conference on Biology, Environment and Chemistry IPCBEE vol.24 IACSIT Press, Singapoore, (2011).

Anirudhan, T. S. and Ramachandran, M., "Removal of 2,4,6-trichlorophenol from water and petroleum refinery industry effluents by surfactant-modified bentonite". Journal of water process engineering, 1: 46-53, 2014.

ASTM D2867-09. (Standard Test Method for Determination of Moisture Content in Activated Carbon

ASTM D4607-14. (Standard Test Method for Determination of Iodine Number of Activated Carbon)

Attia, A. A., Rashwan, W. E., and Khedr, S. A., "Capacity of activated carbon in the removal of acid dyes subsequent to its thermal treatment". Dyes and Pigments. 69:128-136, 2006.

Baker, F. S., Miller, C. E., Repic, A. J. and Tolles, E.D., "Activated carbon. Kirk-Othmer Encycolpedia of Chemical Technology". 4: 1015-1037, 1992.

Bansode, R. R., Losso, J.N., Marshall, W.E., Rao, R.M., and Portier, R.J., "Adsorption Of Volatile Organic Compounds by Pecan Shell and Almond Shell Based Granular Activated Carbons". Bioresource Technology. 90: 175-184, 2003.

Basar, C. A., "Applicability of the various adsorption models of three dyes adsorption onto activated carbon prepared waste apricot". J. Hazard. Mater. B135: 232–241, 2006.

Betiku, E. and Adepoju, T. F., "Methanolysis optimization of beniseed (Sesamum indicum) oil to biodiesel and fuel quality characterization". International Journal of Energy Environmental Engineering, 4: 9-16, 2013.

Buasri, A., Chaiyut, N., Loryuenyong, V., Phakdeepataraphan, E.; Watpathomsub, S., and Kunakemakorn V., "Synthesis of Activated Carbon Using Agricultural Wastes from Biodiesel Production. World Academy of Science, Engineering and Technology International Journal of Chemical, Molecular, Nuclear, Materials and Metallurgical Engineering". 7(1), 2013.

Cunliffe, A.M., and Williams, P. T., "Influence of process conditions on the rate of activation of chars derived from pyrolysis of used tyres". Energy & Fuels. 13(1): 166–175, 1999.

Dada, A. O., Olalekan, A. P., Olatunji, A. M. and Dada, O., "Langmuir, Freundlich, Temkin and Dubinin-Radushkevich isotherm studies of equilibrium sorption of Zinc ion unto phosphoric acid modified rice husk". Journal of Applied Chemistry. 3: 41-42, 2012.

Diao, Y., Walawender, W. P., and Fan, L. T., "Activated Carbons prepared from Phosphoric Acid Activation of Grain Sorghum". Bioresource Technology. 81(1): 45-56, 2002.

Girgis, B.S., Yunis, S.S., and Soliman, A.M., "Characteristics of activated carbon from peanut hulls in relation to conditions of preparation". Materials Letters, 57(1): 164-172,2002.

Gonsalvesh, L., Marinov, S. P., Gryglewicz, G., Carleer, R., and Yperman, J., "Preparation, characterization and application of polystyrene based activated carbons for Ni(II) removal from aqueous solution Fuel Processing Technology". 149: 75–85, 2016.

Hameed, B. H., Ahmad, A. L., and Latiff, K. N. A., "Adsorption of basic dye (methylene blue) onto activated carbon prepared from rattan sawdust". Dyes Pigments, 75:143–149, 2007.

Ho, Y., "Review of second-order models for adsorption systems". Journals of Hazardous materials, 4: 136-681, 2006.

Inamullah, B., Khadija, Q., Kazi, R. A., and Abdul, K. A., "Preparation and characterisation of chemically activated almond shells by optimization of adsorption parameters for removal of chromium (vi) from aqueous solutions". World Academy of Science, Eng. Technol. 34: 199-204, 2008.

La´szlo´, K., Bota, A., and Dekany, I., "Effect of heat treatment on synthetic carbon precursors". Carbon. 41(6):1205–1214, 2003.

Legrouri K., Khouya E., Ezzine M., Hannache H., Denoyel R., Pallier R., and Naslain R., "Production of activated carbon from a new precursor molasses by activation with sulphuric acid". J. Hazard. Mater. 118 (B): 259–263, 2005.

Lian, F., Xing, B., and Zhu, L., "Comparative study on composition, structure, and adsorption behavior of activated carbons derived from different synthetic waste polymers". J Colloid Interface Sci 360 (2):725–730, 2011.

Lua, A. C., and Yang, T., "Characteristics of activated carbon prepared from pistachio-nut shell by zinc chloride activation under nitrogen ad vacuum conditions". Journal of Colloid and Interface Science. 290: 505-513, 2005.

Marsh, H., and Rodríguez-Reinoso, F., "Activated Carbon: Materials & Mechanical". Elsevier Science Ltd. 1: 544 -554, 2006a.

Marsh, H. and Rodríguez-Reinoso, F., "Activation Processes (Thermal or Physical), in Activated Carbon". Elsevier Science Ltd: Oxford. 243-321, 2006b.

Mendez, M. O. A., Lisboa, A. C. L., Coutinhoand, A. R., and Otani, C., "Activated Petroleum Coke for natural gas storage". J. Braz. Chem. Soc., 17(6): 1144-1150, 2006.

Misra, A., Tyagi, P. K., Singh, M. K., and Misra, D. S., "FTIR studies of nitrogen doped carbon nanotubes.Diamond and Related Materials", In Press,Corrected Proof, 2005.

Onal, Y., C. Akmil-Basar, C., Sarıcı, O., and Erdogan S., "Textural development of sugar beet bagasse activated with ZnCl2". J. Hazard. Mater. 142: 138–143, 2007.

Paraskeva, P., Kalderis, D., and Diamadopoulos, E., "Production of activated carbon from agricultural by-products". Journal of Chemical Technology & Biotechnology, 83(5): p. 581-592, 2008.

Park, S. H., McClain, S.; Tian, Z. R., Suib, S. L., and Karwacki, C., "Surface and bulk measurements of metals deposited on activated carbon". Chem Mat. 9: 176-183, 1997.

Prakash Kumar, B. G., Shivakamy, K., Miranda, L. R., and Velan M., "Preparation of steam activated carbon from rubberwood sawdust (Hevea brasiliensis) and its adsorption kinetics". J. Hazard. Mater. B136 (2): 922–929, 2006.

Qiao, W., Yoon, S.H., Korai, Y., Mochida, I., Inoue, S.I., Sakurai, T., and Shimohara, T., "Preparation of activated carbon fibers from polyvinyl chloride". Carbon. 42(7):1327–1331, 2004

Radhika, M., and Palanivelu, K., "Adsorptive removal of chlorophenols from aqueous solution by low cost adsorbent-Kinetics and isotherm analysis". J. Hazard. Mater. 138 (B): 116–124, 2006.

Tan, I. A. W, Hameed, B. H., and Ahmad, A.L., "Equilibrium and kinetic studies on basic dye adsorption by oil palmfibre activated carbon". Chem. Eng. J. 127: 111–119, 2007.

Wang, S. L, Tzou, Y. M., Lu, Y. H., and Sheng, G., "Removal of 3-chlorophenol from water using rice-straw-based carbon". J. Hazard. Mater. 147:313–318, 2007.

Zongxuan J., You, L., Xiuping, Sun., Fuping, T., Fuxia, S., Changhai, L., Wansheng, Y. Chongren. H., and Can, L., "Activated carbon chemically modified by concentrated H_2SO_4 for the adsorption of pollutant from Wastewater and the dibenzothiophene from fuel oils". Langmiur, 19: 731-736, 2003.